

# UC Davis

## UC Davis Previously Published Works

### Title

Late devonian carbon isotope stratigraphy and sea level fluctuations, Canning Basin, Western Australia

### Permalink

<https://escholarship.org/uc/item/6zc2x4rh>

### Journal

Palaeogeography Palaeoclimatology Palaeoecology, 191(2)

### ISSN

0031-0182

### Authors

Stephens, N P  
Sumner, Dawn Y.

### Publication Date

2003-02-01

Peer reviewed



ELSEVIER

Palaeogeography, Palaeoclimatology, Palaeoecology 3024 (2002) 1–17

PALAEO

www.elsevier.com/locate/palaeo

# Late Devonian carbon isotope stratigraphy and sea level fluctuations, Canning Basin, Western Australia

Nat P. Stephens\*, Dawn Y. Sumner

*Department of Geology, University of California, Davis, CA 95616-8605, USA*

Received 16 July 2002; received in revised form 19 November 2002; accepted 10 December 2002

## Abstract

The Upper Devonian reef complexes of the Canning Basin contain some of the world's best exposed, continuous stratigraphic sections through the Frasnian–Famennian boundary. The facies distribution and composition of these reef complexes record interactions among sea level changes, sediment supply, ocean chemistry, and paleoecology. Changes in relative sea level produced spatial shifts in reef platform development and regional changes in sediment supply that can be correlated across facies boundaries using a combination of sequence stratigraphy, biostratigraphy, and carbon isotope stratigraphy. During the lowstand interval below the Frasnian–Famennian boundary, the reef margin advanced down the reef slope in shallow-water environments, and siliciclastics locally dominated in the margin slope environment. Compilation of a broad late Frasnian to early Famennian sequence stratigraphic framework for the Canning Basin demonstrates that transgressive intervals correlate to positive carbon isotopic excursions within the basin. These isotopic shifts also can be correlated to time-equivalent positive carbon isotopic excursions reported from transgressive intervals in Europe. Thus, the late Frasnian transgressions in the Canning Basin were primarily eustatic rather than tectonic in origin, and positive carbon isotopic signatures of the Kellwasser horizons are globally correlative.

© 2002 Published by Elsevier Science B.V.

*Keywords:* Late Devonian; isotopes; Canning Basin; stratigraphy

## 1. Introduction

The use of sequence stratigraphy, chemostratigraphy, and biostratigraphy allows detailed correlation among diverse stratigraphic sections while simultaneously providing insights into critical periods of Earth's history, such as the Late Devonian

an mass extinction. The Frasnian–Famennian boundary marks one of the five major extinctions of the Phanerozoic (Sepkoski, 1996) and has been a major focus of Late Devonian stratigraphic and geochemical studies (Becker et al., 1993; Geldsetzer et al., 1993; Joachimski and Buggisch, 1993; Kennard et al., 1992; Playford et al., 1984; Southgate et al., 1993; Wang et al., 1996; Joachimski et al., 2002). Sea level changes have been proposed as contributing factors to mass extinctions (Copper, 1986; Thompson and Newton, 1988; Joachimski and Buggisch, 1993; Hal-

\* Corresponding author.

E-mail address: [stephens@geology.ucdavis.edu](mailto:stephens@geology.ucdavis.edu) (N.P. Stephens).

43 lam and Wignall, 1999). However, interpretations  
44 of sea level changes across the Frasnian–Famen-  
45 nian boundary vary substantially (Kennard et al.,  
46 1992; George et al., 1997; Hallam and Wignall,  
47 1999).

48 Correlating third-order and higher sea level  
49 changes in the Canning Basin is difficult due to  
50 variations in facies composition, rarity of se-  
51 quence-defining unconformities, and lack of bio-  
52 stratigraphic fossils in shallow reef environments.  
53 Variability in time-equivalent facies can be due to  
54 heterogeneities in reef growth (Ward, 1999) and  
55 localized depocenters of siliciclastics (Holmes and  
56 Christie-Blick, 1993). Correlation of the Kellwasser  
57 horizons of Europe to equivalent strata in the  
58 Canning Basin have not been successful due to a  
59 lack of upper Frasnian black shale horizons in the  
60 Canning Basin (Becker et al., 1991). In the Can-  
61 ning Basin conodont and goniatite biostratigra-  
62 phies have locally provided a basis for regional  
63 and global correlation (Nicoll, 1984; Becker and  
64 House, 1997; George et al., 1997; George and  
65 Chow, 2002). However, these fossils are most  
66 abundant in deep-water facies and rarely found  
67 in back-reef and reef margin environments (Nic-  
68 oll, 1984), which makes biostratigraphic correla-  
69 tion of reef platforms to basinal facies very diffi-  
70 cult if not impossible. Regional and global  
71 correlation of third-order sequences also may be  
72 hampered by local tectonic effects. Hall (1984)  
73 suggested that tectonic activity in the Canning  
74 Basin was locally subsiding by Late Devonian  
75 time. However, Southgate et al. (1993), Holmes  
76 and Christie-Blick (1993), and Ward (1999) cite  
77 tectonic activity as a potential origin for some  
78 of their sequences.

79 Second- and third-order sea level interpreta-  
80 tions for the Upper Devonian reef complexes in  
81 the Canning Basin are based on shifting facies  
82 patterns, rare exposure surfaces, and seismic stra-  
83 tigraphy (Playford et al., 1989; Southgate et al.,  
84 1993; Whittam et al., 1994; George et al., 1997;  
85 Ward, 1999). As a whole, the Upper Devonian  
86 reef complexes of the Canning Basin are inter-  
87 preted as a second-order sequence, because the  
88 reef platforms back-stepped during Frasnian  
89 time and prograded during Famennian time  
90 (Playford, 1980). Although the second-order sea

91 level interpretation is widely accepted, third-order  
92 sequence stratigraphic models are more contro-  
93 versial (Southgate et al., 1993; Holmes and Chris-  
94 tie-Blick, 1993; Whittam et al., 1994; Becker and  
95 House, 1997; George et al., 1997; Ward, 1999).  
96 Based on seismic stratigraphy and well log data,  
97 Southgate et al. (1993) proposed 18 third-order  
98 sequences for upper Devonian to Tournaisian  
99 subsurface strata in the Canning Basin. Becker  
100 and House (1997) also found evidence for sea  
101 level changes in deep-water strata but did not  
102 link these changes to previously interpreted  
103 third-order sequences. Whittam et al. (1994) ex-  
104 tended seven of Southgate et al.'s (1993) subsur-  
105 face sequences to various outcrops in the northern  
106 Canning Basin, using rare exposure surfaces and  
107 shifting facies patterns. Their correlations, how-  
108 ever, have been criticized for lack of time control  
109 (Becker and House, 1997). The subsurface inter-  
110 pretations differ from the third-order sequences  
111 defined by George et al. (1997) for a stratigraphic  
112 section at Dingo Gap. Holmes and Christie-Blick  
113 (1993) and Ward (1999) recognized probable  
114 third-order sequences in the Van Emmerick  
115 Range, at Stony Creek, and in the Napier Range  
116 but expressed uncertainty in correlating their se-  
117 quences to pre-existing sequence stratigraphic  
118 frameworks.

119 Carbon isotope stratigraphy is based on time-  
120 equivalent changes in  $^{13}\text{C}:^{12}\text{C}$  ratios and can serve  
121 as a powerful tool for stratigraphic correlation.  
122 Global changes in the carbon isotopic values of  
123 seawater at the time scale of  $>10^5$  years are due  
124 to long-term variations in carbon burial, conti-  
125 nental weathering, sea surface temperature, and  
126 ocean pH (Lynch-Stieglitz et al., 1995; Spero et  
127 al., 1997; Kump and Arthur, 1999). Shorter-term  
128 variations may be due to fluctuations in primary  
129 productivity, the release of methane clathrates, or  
130 changes in ocean circulation (Kump, 1991; Haq,  
131 1998; Kump and Arthur, 1999; Spero and Lea,  
132 2002). Closed or silled basins, which are not fully  
133 equilibrated with ocean water, may show carbon  
134 isotopic variations independent of the global iso-  
135 topic curve, but basins with good circulation re-  
136 flect global  $\delta^{13}\text{C}$  variations.

137 Thus, carbon isotope stratigraphy provides a  
138 basis for global correlations. For example, Neo-

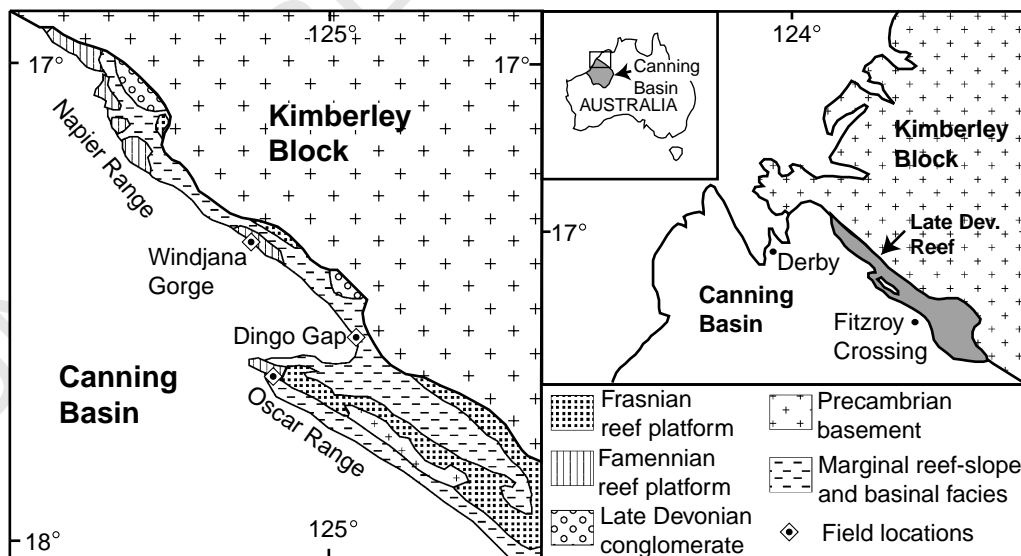
139 proterozoic strata have been correlated using  
 140 large swings in  $\delta^{13}\text{C}$  (Kaufman and Knoll, 1995;  
 141 Hoffman et al., 1998), and  $\delta^{13}\text{C}$  variations have  
 142 been used locally to correlate basinal to reef plat-  
 143 form facies in Cretaceous reef complexes (Grottsch  
 144 et al., 1998; Ferreri, 1997). A  $\delta^{13}\text{C}$  curve for  
 145 upper Frasnian to lower Famennian strata has  
 146 already been defined from European, North  
 147 American, and Australian stratigraphic sections  
 148 (Joachimski and Buggisch, 1993; Wang et al.,  
 149 1996; Joachimski et al., 2002). This  $\delta^{13}\text{C}$  curve  
 150 has two positive excursions and may be used as  
 151 a tool for regional and global stratigraphic correla-  
 152 tion. During Late Devonian time, the Canning  
 153 Basin contained reefs with cosmopolitan fauna,  
 154 suggesting that the water within the basin had  
 155 normal salinity and circulated with the ocean  
 156 (Becker et al., 1991 and references therein). In  
 157 the Canning Basin, carbon isotope curves have  
 158 been measured from deep-water strata at  
 159 McWhae Ridge and Casey Falls and have been  
 160 correlated to Upper Devonian carbon isotope  
 161 curves from Europe and North America (Joa-  
 162 chimski et al., 2002). The  $\delta^{13}\text{C}$  variations ob-  
 163 served from deep-water strata can be used for  
 164 intrabasinal correlation to shallower water facies.

165 This study shows that carbon isotope stratigra-  
 166 phy, accompanied by the available biostratigra-

167 phy and sequence stratigraphy, can serve as a  
 168 powerful tool for stratigraphic correlation in the  
 169 Canning Basin. By using detailed  $\delta^{13}\text{C}$  curves,  
 170 sedimentary indicators of sea level change from  
 171 different locations are correlated to produce a re-  
 172 fined sequence stratigraphic framework for the  
 173 Canning Basin. Carbon isotopic correlations al-  
 174 low comparison of the Canning Basin relative  
 175 sea level curve to late Frasnian–early Famennian  
 176 global sea level interpretations.

## 2. Geologic setting

177  
 178 The northern edge of the Canning Basin was  
 179 located about  $15^\circ$  south of the equator during  
 180 Middle to Late Devonian time and was ideally  
 181 situated for reef building processes (Playford,  
 182 1980; Hurley, 1986). Termed the Devonian ‘Great  
 183 Barrier Reef’, the 350-km northwest–southeast-  
 184 trending Givetian to Famennian reef complexes  
 185 provide an unparalleled view of Late Devonian  
 186 reef life and reef development (Fig. 1). During  
 187 Late Devonian time, the Canning Basin was an  
 188 extensional basin with high subsidence rates  
 189 (Holmes and Christie-Blick, 1993; Southgate et  
 190 al., 1993) that accommodated over 2 km of De-  
 191 vonian strata (Brown et al., 1984).



1 Fig. 1. Location and general geology of field area. Modified from Kerans et al. (1986).

192 Stratigraphic nomenclature for division of reef  
 193 facies was defined by Guppy et al. (1958), Play-  
 194 ford and Lowry (1966), and Playford (1980). Plat-  
 195 form facies are recognized as horizontal beds of  
 196 mostly carbonate in a shallow-water depositional  
 197 environment. The reef margins are discontinuous,  
 198 massively bedded framestones and bindstones at  
 199 the edge of the reef platforms. Marginal slope  
 200 facies are recognized by steep depositional dips  
 201 and are situated between platform and basinal  
 202 facies. Frasnian platform facies comprise the Pil-  
 203 lara Formation (Playford, 1980). The back-reef  
 204 subfacies of the Famennian platform strata are  
 205 the Nullara Formation, and Famennian reef mar-  
 206 gin and reefal slope subfacies comprise the Wind-  
 207 jana Limestone (Playford, 1980). The Napier For-  
 208 mation is composed of both Frasnian and  
 209 Famennian marginal slope strata (Playford,  
 210 1980).

### 211 3. Methods

212 Three areas were examined for this study, the  
 213 Oscar Range, Windjana Gorge, and Dingo Gap  
 214 (Fig. 1). Long stratigraphic sections (>100 m)  
 215 were measured for broad trends in sedimentology  
 216 and carbon isotopic values. Shorter sections were  
 217 measured at specific areas of interest. Available  
 218 biostratigraphic and sequence stratigraphic data  
 219 were used for preliminary stratigraphic correla-  
 220 tion. At Windjana Gorge a 245-m section was  
 221 measured at the eastern end of the gorge and a  
 222 44-m section was measured across the Frasnian–  
 223 Famennian boundary in the ‘classic face’ area of  
 224 the gorge (Playford, 1980). At Dingo Gap, the  
 225 lower part of George et al.’s (1997) section was  
 226 remeasured to produce a 236-m section, and a 57-  
 227 m section was measured in the Dingo Gap back-  
 228 reef area, described by Ward (1996, 1999). At the  
 229 northwestern tip of the Oscar Range, two strati-  
 230 graphic sections were measured and combined to  
 231 form a 106-m section. In all stratigraphic sections,  
 232 samples were collected at regular intervals of  
 233 about 10 m with higher-density sampling around  
 234 the Frasnian–Famennian boundary.

### 3.1. Laboratory methods

235 Samples collected from the field were made into  
 236 thin sections and were screened with both stan-  
 237 dard and cathodoluminescent microscopy.  $\delta^{13}\text{C}$   
 238 sampling focussed on micrites, early marine ce-  
 239 ments, and brachiopods with well-preserved pet-  
 240 rographic textures and little to no luminescence.  
 241 In peloidal packstones and wackestones, micrite  
 242 samples were obtained from clusters of micritic  
 243 peloids within a micrite matrix.  $\delta^{13}\text{C}$  values asso-  
 244 ciated with siliciclastic-rich strata were obtained  
 245 from brachiopods and peloidal grainstone–pack-  
 246 stone beds intercalated within the sandier litho-  
 247 facies. Early marine cements, such as radiaxial  
 248 fibrous calcites and fine-bladed calcites, were  
 249 sampled where available. Powders for carbon iso-  
 250 tope analyses were drilled either from thin section  
 251 billets using a standard drill press with a 0.75-mm  
 252 diamond drill bit or from thin sections using an  
 253 automated Merchantek microdrill with a 10- $\mu\text{m}$   
 254 drill tip. Samples were roasted under vacuum  
 255 for 1 h at 350°C in order to remove organic car-  
 256 bon. Stable isotope analyses were performed on a  
 257 Fisons Optima isotope ratio mass spectrometer  
 258 using an Isocarb common acid bath at 90°C at  
 259 the University of California, Davis. Analytical  
 260 precision of both carbon and oxygen isotopic  
 261 analyses is better than  $\pm 0.1\%$  (2 $\sigma$ ).  $\delta^{13}\text{C}$  and  
 262  $\delta^{18}\text{O}$  values are reported relative to VPDB.  
 263

## 4. Results and interpretations

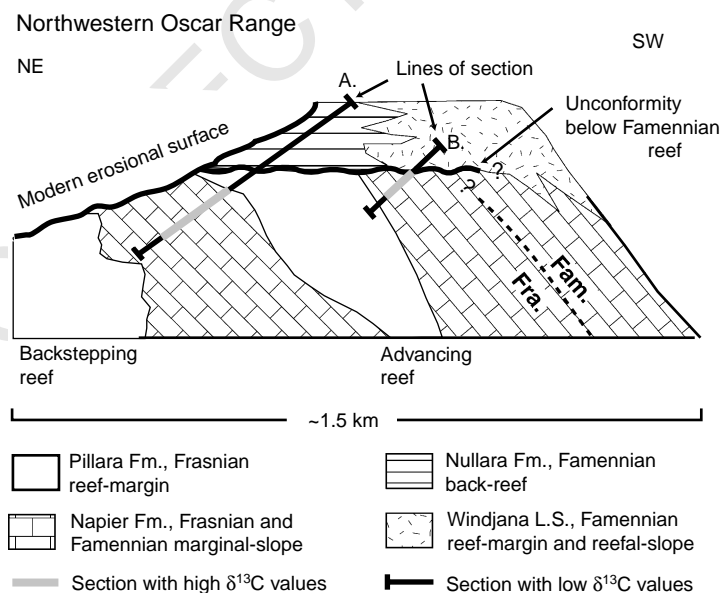
### 4.1. Sedimentology

264 The long stratigraphic sections of this study,  
 265 measured at Dingo Gap, eastern Windjana  
 266 Gorge, and the Oscar Range, can be roughly cor-  
 267 related using regional facies tracts and biostratig-  
 268 raphy. The late Frasnian reefs in the Napier  
 269 Range developed as three back-stepping plat-  
 270 forms, which can be correlated regionally  
 271 (Ward, 1999). The long sections at Windjana  
 272 Gorge and Dingo Gap begin in or on top of  
 273 Ward’s (1999) platform B. The long section  
 274 from the Oscar Range begins at the second to  
 275 last reef platform identified by Hurley (1986).  
 276  
 277

278 This reef platform also has a back-stepping mor-  
 279 phology and may correlate to platform B in the  
 280 Napier Range. The three long sections and the  
 281 classic face section pass through the Frasnian–Fa-  
 282 mennian boundary. In the Windjana Gorge east  
 283 and classic face sections, conodont dating identi-  
 284 fies the Frasnian–Famennian boundary within a  
 285 0.5-m interval (P. Playford, 1999, personal com-  
 286 munication). Conodont dating from the Dingo  
 287 Gap section places the Frasnian–Famennian  
 288 boundary within a 7-m interval (George et al.,  
 289 1997), and the Frasnian–Famennian boundary in  
 290 the Oscar Range is placed at an unconformity  
 291 that truncates beds containing the last occurrence  
 292 of Frasnian stromatoporoids (Hurley, 1986).

293 The northwestern Oscar Range has excellent  
 294 exposures of upper Frasnian and lower Famen-  
 295 nian strata. In the outcrops where sections were  
 296 measured, Famennian strata grade laterally from  
 297 back-reef to reef margin facies. An unconformity  
 298 is present at the Frasnian–Famennian boundary  
 299 in the Oscar Range and in some locations is re-  
 300 ported to have physical relief of at least 1–2 m  
 301 (Hurley, 1986). The northern Oscar Range has

302 very little siliciclastic sediment, possibly due to  
 303 paleogeographic separation of the reef from the  
 304 mainland (Playford et al., 1989), (Fig. 1). Based  
 305 on reef geometries, Hurley (1986) classified the  
 306 two Frasnian reef platforms observed in this  
 307 study as back-stepping and advancing (Fig. 2).  
 308 In the Oscar Range section (Fig. 2), Frasnian  
 309 strata consist of alternating reef platforms and  
 310 intervals of upper marginal slope facies. The Fra-  
 311 snian reef platforms are massively bedded, stroma-  
 312 toporoid framestones with some corals, some bra-  
 313 chiopods, and abundant renalcids. Both massive  
 314 and branching stromatoporoids were observed,  
 315 and many are in up-right growth position. The  
 316 Frasnian upper marginal slope facies consist of  
 317 medium to thickly bedded, peloidal grainstones  
 318 and packstones, containing transported stroma-  
 319 toporoids, brachiopods, crinoids, sponges, and  
 320 rare nautiloids. Depositional dips of these beds  
 321 were approximately 25°, based on geopetal indi-  
 322 cators of stratigraphic up. In some cases, filamen-  
 323 tuous algal fossils are observed and probably  
 324 bound the marginal slope sediment. Famennian  
 325 back-reef strata are well bedded, peloidal grain-



1 Fig. 2. Interpretive diagram of reef complex at northwestern tip of Oscar Range. Reefs were interpreted as advancing and back-  
 2 stepping by Hurley (1986). Strata in section B contain an interval of high  $\delta^{13}\text{C}$  values, which are missing from section A. Sec-  
 3 tions A and B were combined for Figs. 5 and 6. Position of the unconformity and placement of the Frasnian–Famennian bound-  
 4 ary in the marginal slope strata are uncertain.

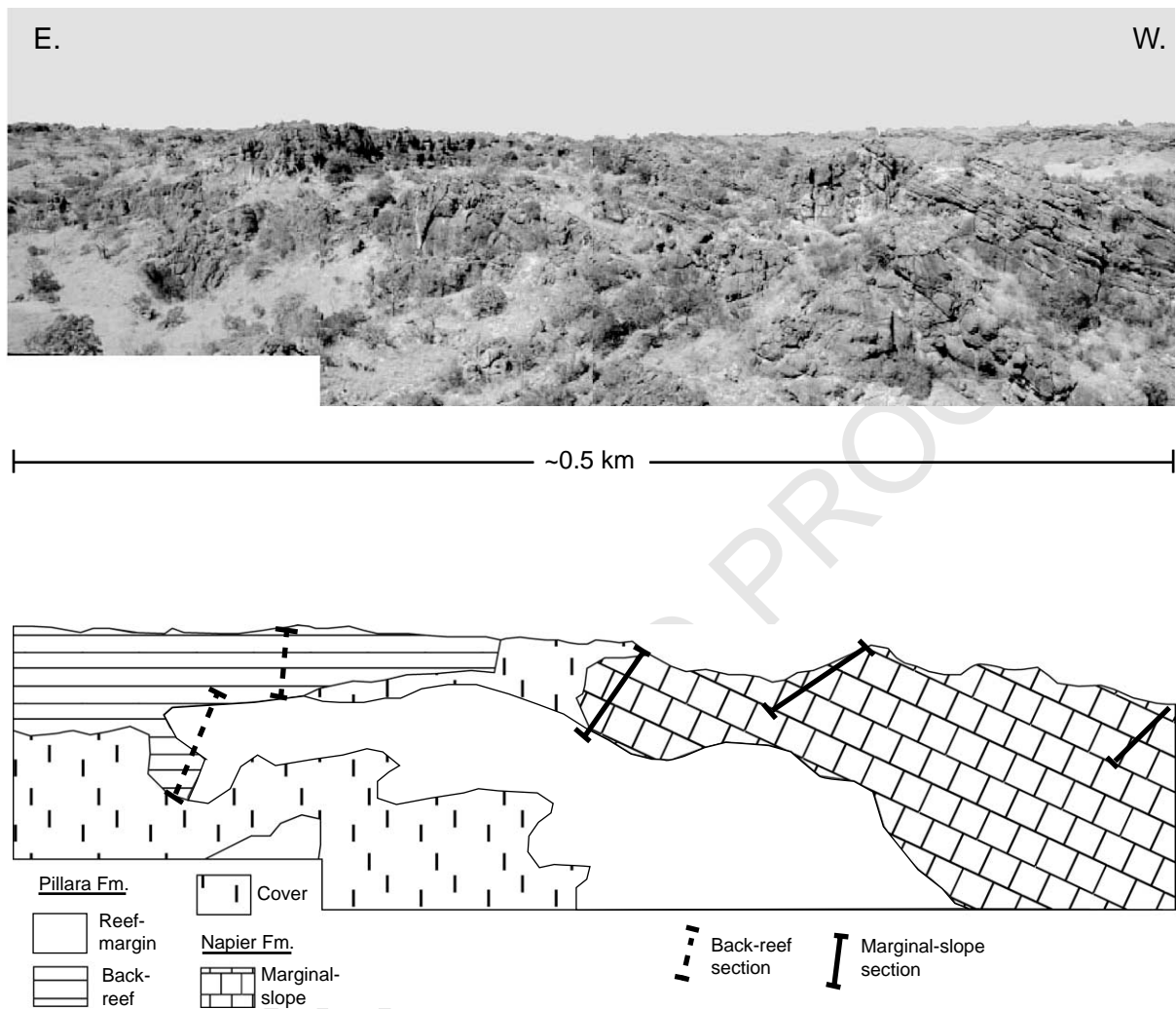
stones and wackestones with ooids, oncoids, and fenestral porosity. Famennian reef margin and reef flat rocks consist of massively bedded, microbial bindstones and framestones.

The back-reef section measured at Dingo Gap spans a back-stepping interval identified by Ward (1999) (Fig. 3). In the back-reef strata, beds alternate between stromatoporoid framestones, peloidal grainstones, and fenestral wackestones in 2–4-m shallowing upward intervals. These strata are similar to those described at Windjana Gorge by Wood (2000) and in the Pillara Range by Read (1973). The middle of the Dingo Gap back-reef section is interrupted by reef margin facies, which consists of massively bedded stromatoporoid framestones. These beds are difficult to trace laterally and may be composed of multiple isolated bioherms. Above the bioherms, marginal slope strata onlap the reef margin subfacies, and the reef platform has a back-stepping morphology (Fig. 3).

Stratigraphic sections through marginal slope facies were measured at Dingo Gap and Windjana Gorge. Measured depositional dips of these beds vary from 15° to 45° (Playford and Hocking, 1999). The Dingo Gap marginal slope section starts in the Frasnian reef margin at a stratigraphic horizon, which can be physically traced to the Dingo Gap back-reef section (Fig. 3). Stratigraphically above the reef margin lie approximately 30 m of coarse reef breccias, which have been interpreted as a product of reef collapse (George et al., 1997). Near the Frasnian–Famennian boundary, several bioherms and/or allochthonous reef blocks are associated with beds of grainstone and reef breccia, which correspond to George et al.'s (1997) lithofacies one. George et al. (1997) describe a large bioherm below the Frasnian–Famennian boundary, which consists of corals, sponges, and stromatoporoids. However, many large blocks above and adjacent to this bioherm have geopetal indicators suggesting transport. Many of the allochthonous blocks and/or bioherms are topped by in situ deep-water stromatolites (George, 1999). A prominent 2 m thick, brachiopod rudstone passes just below the Frasnian–Famennian boundary and is laterally traceable along strike for at least 100 m in both directions. The lower Famennian strata of the Dingo Gap

section grade from packstones and grainstone to coarse quartzofeldspathic sandstone. The slightly sandy, thinly bedded, oolitic grainstones correspond to George et al.'s (1997) lithofacies two, and the carbonate-rich strata in the marginal slope section at Dingo Gap comprise the Kalmanyi Member of the Napier Formation (Playford and Hocking, 1999). At the top of the section, sandstone beds, with some ooid-rich intervals and allochthonous reef blocks, correspond to the base of the Tarakalu Member of the Napier Formation (Playford and Hocking, 1999) and George et al.'s (1997) lithofacies three. Locally, the brachiopod-rich bed, allochthonous blocks, and bioherms were partially dolomitized.

Two marginal slope sections were measured at Windjana Gorge, a long section at the eastern end and a short section across the Frasnian–Famennian boundary in the 'classic face'. At the eastern end of Windjana Gorge, the marginal slope strata consist of alternating carbonate and siliciclastic intervals (Fig. 4). The base of the eastern section begins in reef platform B (Ward, 1996), which is stromatoporoid framestone with some sponges and renalcids. The reef platform is overlain by approximately 15 m of coarse reef breccia. Of the two major carbonate-rich intervals, a 50-m interval lies above the coarse reef breccia, and a 35-m interval spans the Frasnian–Famennian boundary. They consist of packstones and grainstones with some thin reef breccia beds. The siliciclastic beds consist of siltstones and very fine quartzofeldspathic sandstones with occasional 0.5–1 m thick interbeds of reef breccia. Large allochthonous reef blocks and possibly some bioherms also are present near the Frasnian–Famennian boundary. The allochthonous reef blocks are angular and have geopetal indicators suggesting transport. A brachiopod rudstone lies just under the Frasnian–Famennian boundary. The rudstone consists of several brachiopod-rich lenses and has a composition similar to the brachiopod rudstone from Dingo Gap. Above the brachiopod rudstone, a 2 m thick bed of red siltstone/fine sandstone contains possible stromatolites. At the Frasnian–Famennian boundary, no evidence for an unconformity exists in marginal slope subfacies at Windjana Gorge. Famennian strata grade



1

Fig. 3. Photomosaic and sketch of strata at Dingo Gap. See Figs. 5 and 6 for stratigraphic columns.

422 from peloidal grainstone and packstones to coarse  
 423 quartzofeldspathic sandstones. The sandstone  
 424 beds at the top of the eastern Windjana Gorge  
 425 section are stratigraphically equivalent to the Tar-  
 426 akalu Member at Dingo Gap.

427 In the 'classic face' section, the strata are al-  
 428 most entirely carbonates and do not contain the  
 429 thick intervals of siliciclastic strata observed in the  
 430 eastern section. The Frasnian–Famennian bound-  
 431 ary is at the contact of a brachiopod rudstone and  
 432 a recessive 0.5 m thick siltstone. A bioherm or  
 433 allochthonous block also is present just below

434 the Frasnian–Famennian boundary in the classic  
 435 face section. Patchy dolomitization was observed  
 436 locally in both Windjana Gorge sections. Gener-  
 437 ally, the limestone is well preserved and usually  
 438 non-luminescent in thin section.

#### 4.2. Stratigraphic interpretation

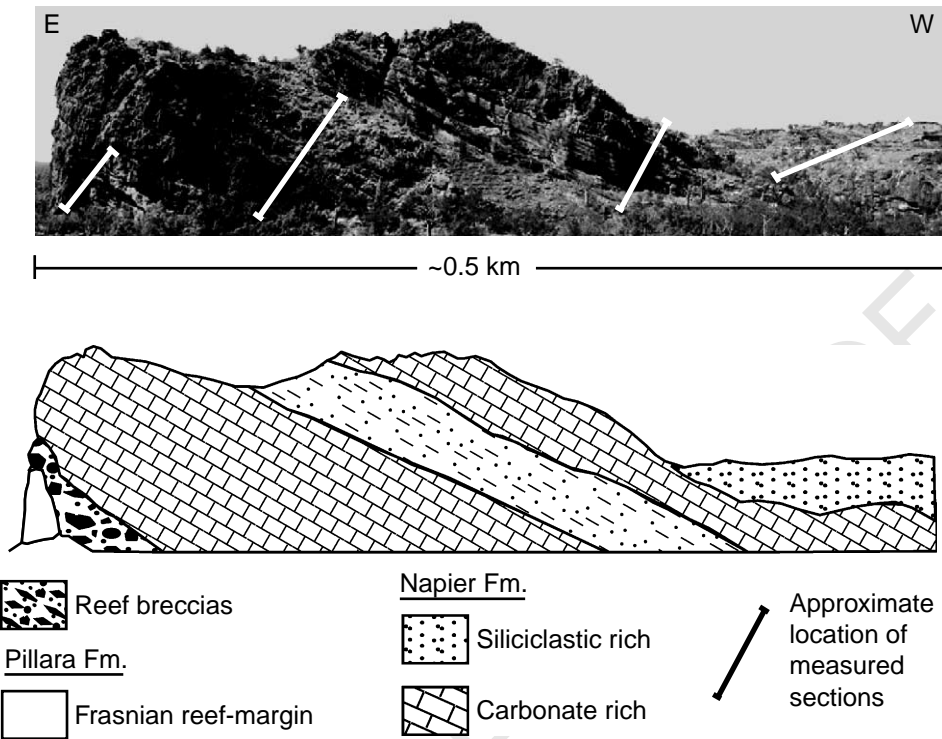
439  
 440 In the measured sections, variations in facies  
 441 composition and spatial shifts of facies through  
 442 time are the basis for interpretations of sea level  
 443 fluctuations. Sequence stratigraphic models of reef

434  
435  
436  
437  
438

439

440  
441  
442  
443



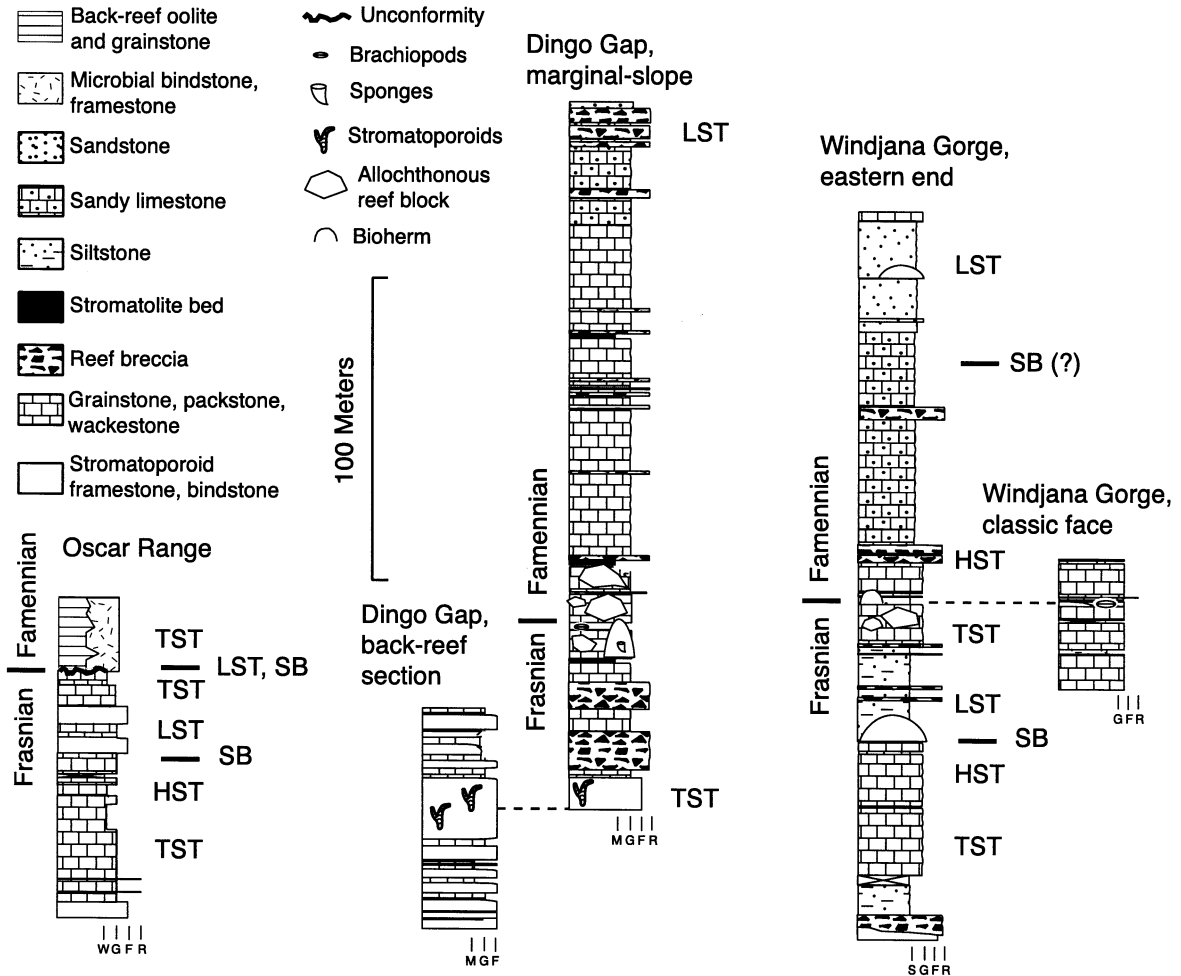


1 Fig. 4. Photomosaic and sketch of strata at the eastern end of Windjana Gorge. See Figs. 5 and 6 for stratigraphic columns.

444 development predict that the position of the reef  
 445 margin changes with respect to fluctuations in rela-  
 446 tive sea level (Handford and Loucks, 1993).  
 447 Therefore, alternating intervals of reef margin  
 448 and upper marginal slope facies at the northwest-  
 449 ern tip of the Oscar Range are interpreted as sea-  
 450 level-driven (Figs. 2 and 5). In the stratigraphic  
 451 column, reef margin facies represent highstand to  
 452 lowstand conditions, and upper reef slope facies  
 453 represent two late Frasnian transgressive intervals.  
 454 A sequence boundary corresponds to the  
 455 Frasnian–Famennian boundary in the Oscar  
 456 Range, and a second sequence boundary is inter-  
 457 preted below a lowstand reef margin (Fig. 5).  
 458 Back-stepping events in the Frasnian reef plat-  
 459 form at Dingo Gap and Windjana Gorge also  
 460 were due to rises in relative sea level (Playford  
 461 et al., 1989; Ward, 1999). Similar sea-level-driven  
 462 facies patterns have been observed in the Tertiary  
 463 reef strata of the Bahamas platform margin,  
 464 where prograding reef framestones correspond to  
 465 lowstand to highstand conditions and are overlain

466 by transgressive upper marginal slope strata  
 467 (Kenter et al., 2001).

468 In the marginal slope facies, changes in lithol-  
 469 ogy may reflect changes in relative sea level. Re-  
 470 ciprocal carbonate–siliciclastic sedimentation at  
 471 the eastern end of Windjana Gorge is interpreted  
 472 as sea-level-driven. Sequence stratigraphic models  
 473 predict that during transgressive to highstand in-  
 474 tervals siliciclastic sediments are deposited farther  
 475 shoreward on the shelf and carbonate sedimenta-  
 476 tion dominates the reef slope (Handford and  
 477 Loucks, 1993). Conversely, during lowstand con-  
 478 ditions the carbonate factory shuts down, silici-  
 479 clastic sediments breach the reef platforms, and  
 480 siliciclastic deposition dominates the reef slopes  
 481 (Handford and Loucks, 1993). Based on seismic  
 482 stratigraphy and core logs, reciprocal sedimenta-  
 483 tion is documented in subsurface stratigraphy in  
 484 the Canning Basin (Southgate et al., 1993).  
 485 Holmes and Christie-Blick (1993) have observed  
 486 possible evidence for reciprocal sedimentation in  
 487 outcrop in the Van Emmerick Range and at



1 Fig. 5. Stratigraphic columns from Canning Basin and sea level interpretations based on facies relationships and facies composition  
 2 (see Figs. 1–4 for locations of sections). TST—transgressive system tract, HST—highstand system tract, LST—lowstand system  
 3 tract, R—reef breccia, F—framestone, G—packstone/grainstone, W—micrite/wackestones, S—siltstones, M—mudstones.

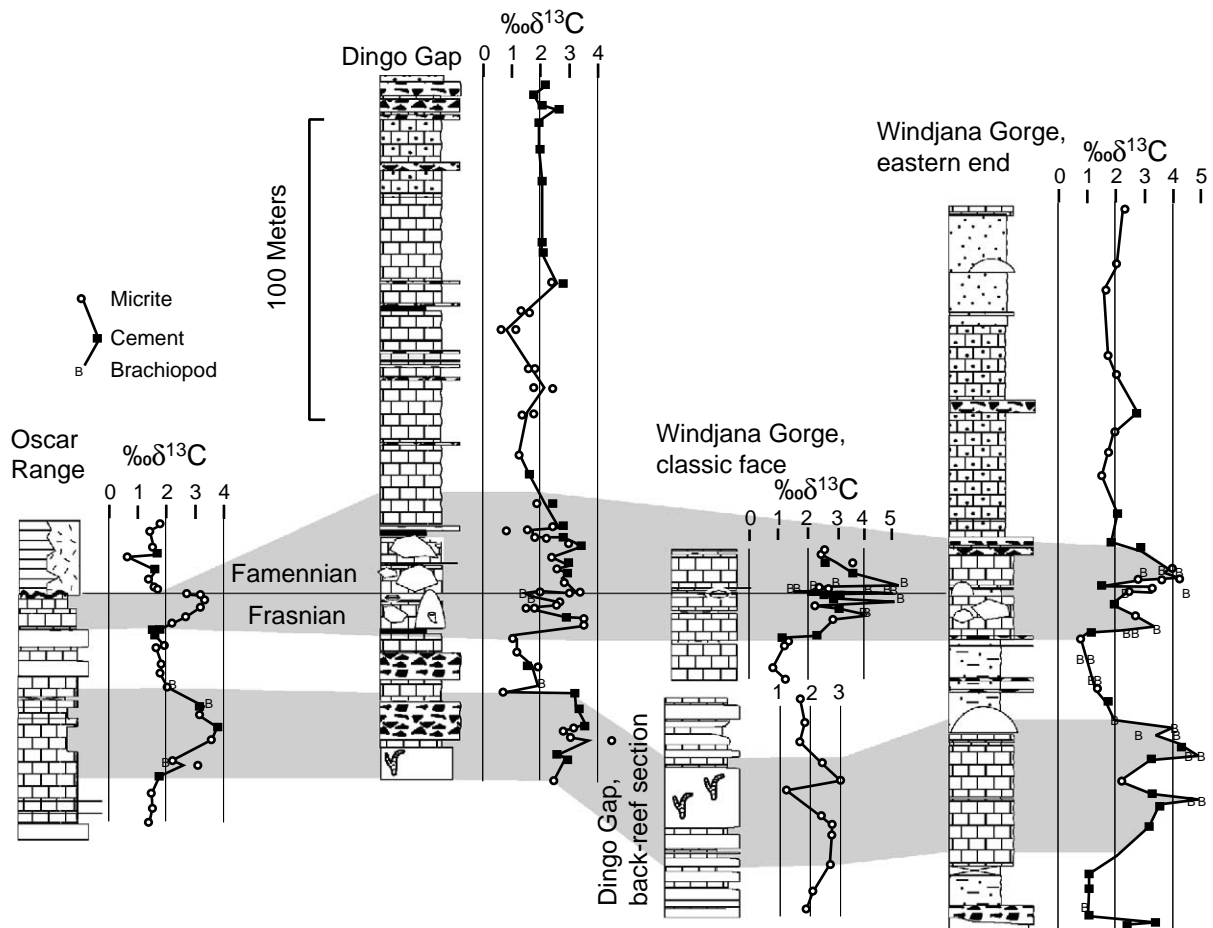
488 Stony Creek in the Canning Basin. At Dingo  
 489 Gap, [George et al. \(1997\)](#) interpreted the transition  
 490 from the carbonate-rich strata to the silici-  
 491 clastic-rich strata in the Famennian as the result  
 492 of a transition from highstand to lowstand con-  
 493 ditions. Although siliciclastic sedimentation in a  
 494 reef complex can be highly variable, the alternat-  
 495 ing carbonate and siliciclastic intervals at the east-  
 496 ern end of Windjana Gorge are probably the re-  
 497 sult of sea-level-driven reciprocal sedimentation  
 498 ([Fig. 5](#)).

### 4.3. Results of carbon isotope geochemistry

499

The  $\delta^{13}\text{C}$  curves for all stratigraphic sections  
 have average baseline values of +1–+2‰ and  
 positive excursions with  $\delta^{13}\text{C}$  values ranging up  
 to +6‰ ([Fig. 6](#)). The magnitude of the positive  
 excursions varies among sections and may be a  
 function of the material sampled with the most  
 positive  $\delta^{13}\text{C}$  values corresponding to brachio-  
 pods. The Dingo Gap and eastern Windjana  
 Gorge sections have two broad, positive carbon  
 isotopic excursions, one spanning 25 m across the  
 Frasnian–Famennian boundary and a second be-

500  
 501  
 502  
 503  
 504  
 505  
 506  
 507  
 508  
 509  
 510



1 Fig. 6. Carbon isotopic correlation of Canning Basin sections. Where more than one data point exists for sampling horizon, carbon isotope curve is drawn through average of points. Gray field correlates positive carbon isotope excursions. See Fig. 5 for stratigraphic symbols and Figs. 1–4 for section locations.

511 tween 40 and 80 m below the Frasnian–Famennian boundary (Fig. 6). In the eastern Windjana  
 512 Gorge section, the positive  $\delta^{13}\text{C}$  excursions correspond to the more carbonate-rich intervals. Most  
 513 of the Dingo Gap back-reef section consists of a positive excursion. The Oscar Range section contains two positive excursions, which lie 30–60 and  
 514 0–8 m below the Frasnian–Famennian boundary and occur in upper reef slope facies (Fig. 6). Unlike the other sections, the Oscar Range section  
 515 does not show a positive  $\delta^{13}\text{C}$  excursion in the earliest preserved Famennian strata (Fig. 6).  
 516 Within the positive  $\delta^{13}\text{C}$  excursions at Windjana Gorge and Dingo Gap, several sharp negative ex-

525 cursions drop to baseline values and are typically  
 526 represented by one or two data points. One of  
 527 these negative excursions is just below the Frasnian–Famennian boundary.  
 528

#### 4.4. Diagenesis

529  
 530 The isotopic trends observed in the  $\delta^{13}\text{C}$  curves  
 531 are considered primary features based on petrography, luminescence, and  $\delta^{18}\text{O}$  values (cf. Kerans  
 532 et al., 1986; Hurley and Lohmann, 1989). Petrographically, neither the early marine cements nor  
 533 the micrites show significant recrystallization. All  
 534 analyzed brachiopods have well-preserved shell  
 535

537 textures. The well-preserved petrographic textures  
 538 of the micrites, early marine cements, and bra-  
 539 chiopods suggest that major diagenetic alteration  
 540 did not occur. Thin sections were screened for  
 541 luminescence, which is caused by the diagenetic  
 542 replacement of calcium in the calcite with manga-  
 543 nese and iron. The samples chosen for stable iso-  
 544 tope analyses were slightly luminescent to non-lu-  
 545 minescent, which suggests little manganese  
 546 substitution alteration. Carbon and oxygen iso-  
 547 topes in the stratigraphic sections lack typical  
 548 trends attributed to diagenesis (cf. Hurley and  
 549 Lohmann, 1989) (Fig. 7). The isotopic composi-  
 550 tions of non-luminescent and slightly luminescent  
 551 brachiopods, micrites, and cements overlap and  
 552 lack correlations to manganese concentrations  
 553 (data not shown). The lack of correlation of  
 554  $\delta^{13}\text{C}$  values to sample type, luminescence, or  
 555  $\delta^{18}\text{O}$  values suggests the  $\delta^{13}\text{C}$  shifts were not  
 556 due to diagenesis. In addition, the broad  $\delta^{13}\text{C}$   
 557 trends are reproducible in all sections, regardless

of the lithologic differences between the sections.  
 Thus, the broad  $\delta^{13}\text{C}$  trends are almost certainly  
 original.

#### 4.5. Carbon isotope stratigraphy

The broad trends in the  $\delta^{13}\text{C}$  curves are inter-  
 preted as global and can be used for correlation  
 of strata in the Canning Basin. The Canning Ba-  
 sin had open circulation with seawater (Carpenter  
 et al., 1991), and all sections measured were in the  
 mixed layer of the water column and should not  
 show isotopic anomalies due to basinal stratifica-  
 tion. Global correlations based on the available  
 biostratigraphic data from Dingo Gap, Europe,  
 and Canada consistently show two positive  $\delta^{13}\text{C}$   
 excursions in the upper *rhenana* to *linguiformis*  
 biozones confirming that the  $\delta^{13}\text{C}$  excursions are  
 global signatures (Fig. 8) (Joachimski and Bug-  
 gisch, 1993; Wang et al., 1996). Thus, the upper  
 Frasnian to lower Famennian strata with the pos-

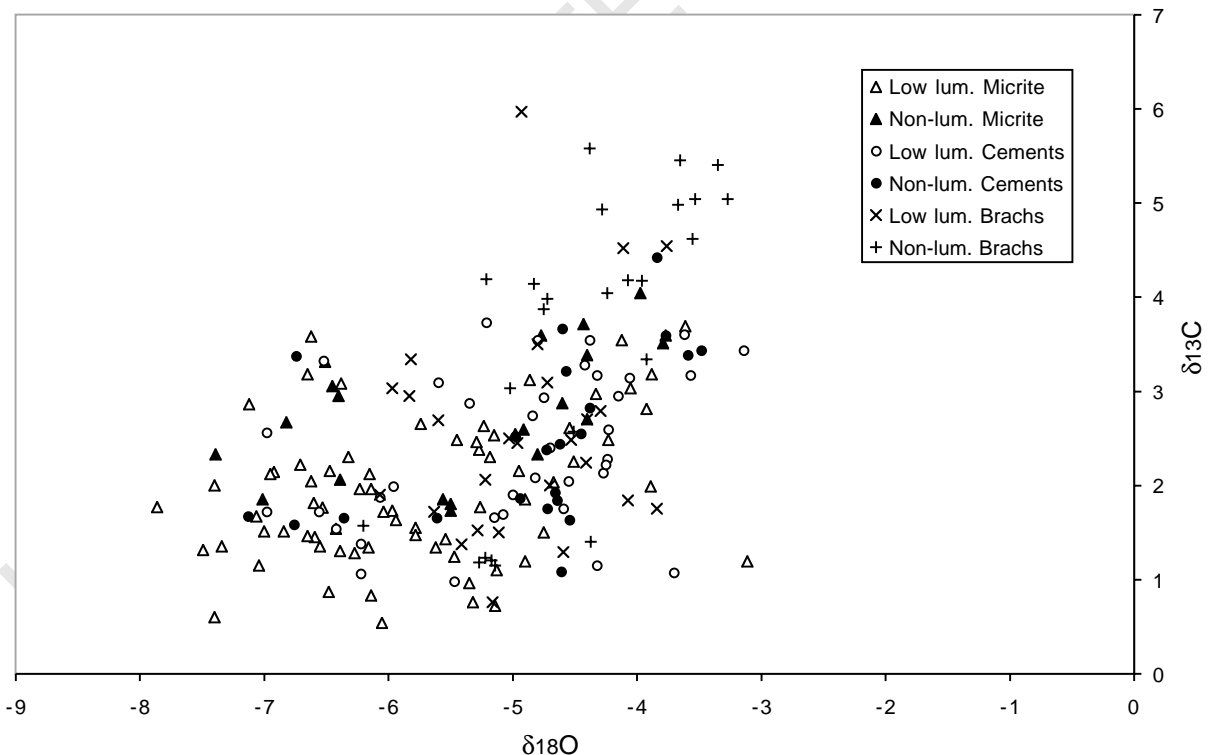


Fig. 7. Carbon and oxygen isotopic values of samples used for  $\delta^{13}\text{C}$  correlations.

577 itive carbon isotope excursion were deposited at  
578 the same time.

579 The lower positive  $\delta^{13}\text{C}$  excursion correlates  
580 transgressive intervals at Dingo Gap, Oscar  
581 Range, and Windjana Gorge (Figs. 5 and 6).  
582 The back-stepping reef platform from the Oscar  
583 Range and platform B in the Napier Range are  
584 below the lower positive  $\delta^{13}\text{C}$  excursions, suggest-  
585 ing that these back-stepping events were roughly  
586 synchronous in the Oscar and Napier Ranges  
587 (Fig. 6). The positive  $\delta^{13}\text{C}$  excursion corresponds  
588 to a deepening depositional environment in the  
589 Oscar Range, an aggrading and back-stepping  
590 reef platform at Dingo Gap, and a carbonate-  
591 rich interval in the marginal slope strata at Wind-  
592 jana Gorge. Based on sedimentary indicators of  
593 sea level change, a transgression occurred at the  
594 three locations in the Canning Basin during the  
595 lower positive  $\delta^{13}\text{C}$  excursion.

596 Between the upper and lower positive  $\delta^{13}\text{C}$  ex-  
597 cursions, the sedimentary indicators of sea level at  
598 the Oscar Range and Windjana Gorge suggest a  
599 drop in sea level. During this interval, the advanc-  
600 ing reef margin in the Oscar Range corresponds  
601 to the late Frasnian siliciclastic interval at Wind-  
602 jana Gorge. The reef breccias at Dingo Gap are  
603 somewhat ambiguous as to whether they formed  
604 during a transgression or regression (George et  
605 al., 1997). However, by correlating the low  $\delta^{13}\text{C}$   
606 interval at Dingo Gap to the Oscar Range sec-  
607 tion, the breccias can be interpreted as initiating  
608 during a highstand and continuing into a low-  
609 stand (Fig. 6).

610 The upper positive carbon isotopic excursion  
611 correlates transgressive, upper marginal slope  
612 strata in the Oscar Range with carbonate-rich in-  
613 tervals in both Windjana Gorge and Dingo Gap.  
614 George et al. (1997) also interpreted parts of this  
615 interval as transgressive at Dingo Gap. Based on  
616  $\delta^{13}\text{C}$  correlation with the Oscar Range and Dingo  
617 Gap, the origin of the reciprocal carbonate–sili-  
618 clastic sedimentation at Windjana Gorge can be  
619 confirmed as sea-level-driven. Stratigraphically  
620 above the upper positive  $\delta^{13}\text{C}$  excursion, the stra-  
621 ta at both Windjana Gorge and Dingo Gap grade  
622 from carbonates to siliciclastics, suggesting a drop  
623 in sea level at both locations, based on models of  
624 reciprocal sedimentation. For much of the Fa-

625 mennian strata, the carbon isotopic curves are  
626 consistently at baseline values of around 2‰,  
627 which correspond to the lack of transgressive in-  
628 tervals in the lower Famennian.

629 At Dingo Gap and Windjana Gorge, sharp de-  
630 creases in  $\delta^{13}\text{C}$  punctuate the broad positive  $\delta^{13}\text{C}$   
631 excursions and may represent either remixing of  
632 older sediment or short-term fluctuations in the  
633 carbon cycle. Mass wasting of the reefs created  
634 reef breccia beds and allochthonous reef blocks  
635 in the marginal slope and may have mixed car-  
636 bonate material with varying original  $\delta^{13}\text{C}$  values.  
637 Brief changes in ocean chemistry and ocean circula-  
638 tion also can produce sharp negative  $\delta^{13}\text{C}$  ex-  
639 cursions (Kump, 1991; Spero and Lea, 2002),  
640 which may be superimposed on the broad positive  
641  $\delta^{13}\text{C}$  excursion of the Late Devonian. Also, vari-  
642 able  $\delta^{13}\text{C}$  values within a stratigraphic horizon  
643 may be explained by changes in the  $\delta^{13}\text{C}$  value  
644 of seawater during the intervals between micrite  
645 formation, brachiopod growth, and cementation  
646 of the voids. However, the identification of a  
647 sharp negative  $\delta^{13}\text{C}$  excursion as mixing of sedi-  
648 ment or a short-term change in ocean chemistry  
649 can be difficult. The negative  $\delta^{13}\text{C}$  excursion just  
650 below the Frasnian–Famennian boundary at  
651 Windjana Gorge may represent a short-term  
652 change in ocean chemistry (Fig. 6), because low  
653  $\delta^{13}\text{C}$  brachiopods at the Frasnian–Famennian  
654 boundary have both valves intact and do not ap-  
655 pear abraded, suggesting very little syndeposition-  
656 al transport.

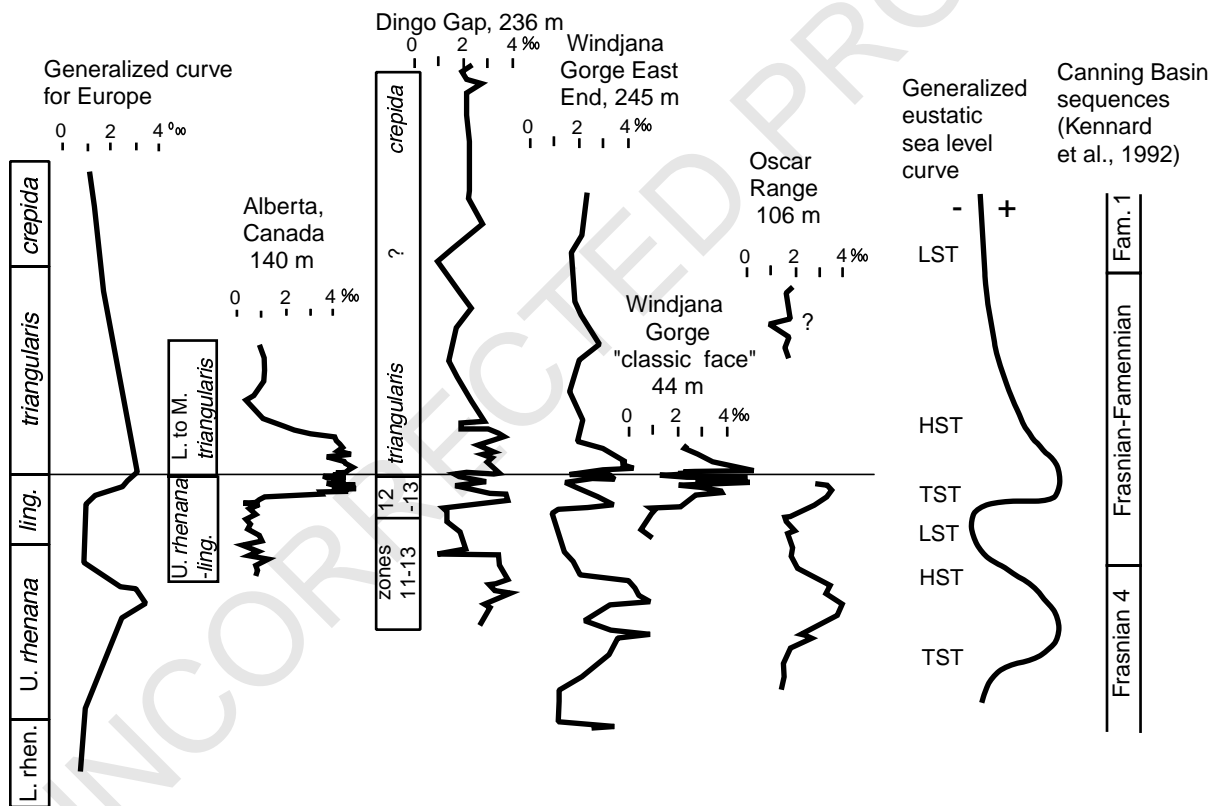
## 657 5. Discussion

658 In addition to the sequence stratigraphy and  
659 biostratigraphy, carbon isotope stratigraphy pro-  
660 vides a way of correlating time-equivalent upper  
661 Frasnian to lower Famennian strata. This corre-  
662 lation can extend sequence stratigraphic interpre-  
663 tations and help differentiate eustatic versus tec-  
664 tonic subsidence. We interpret changes in sea level  
665 in the Canning Basin as eustatic in origin, based  
666 on correlations of  $\delta^{13}\text{C}$  fluctuations (Fig. 8). In  
667 the Canning Basin and Europe, transgressive in-  
668 tervals correspond to positive  $\delta^{13}\text{C}$  excursions. In  
669 Europe, the positive  $\delta^{13}\text{C}$  excursions are found

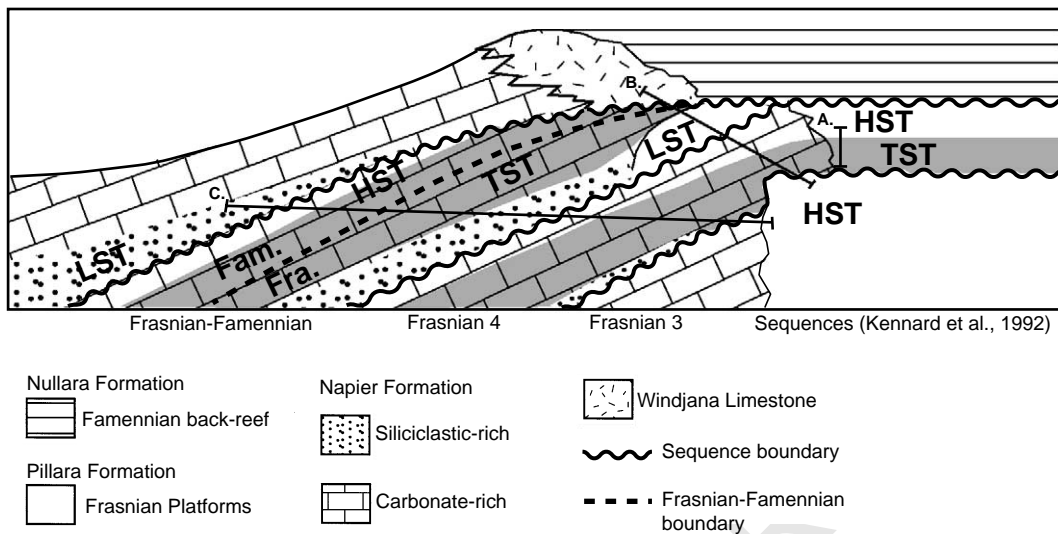
670 within the transgressive Kellwasser horizons (Joachimski and Buggisch, 1993). The late Frasnian to  
 671 early Famennian transgressions occurred at the same time in Europe and Australia and are al-  
 672 most certainly eustatic in origin. Although the Canning Basin was tectonically active during De-  
 673 vonian time, eustatic fluctuations were superimposed on tectonic subsidence and were largely re-  
 674 sponsible for changes on facies composition and distribution in the upper Frasnian and lower Fa-  
 675 mennian Canning Basin. Although the Canning Basin was tectonically active during De-  
 676 vonian time, eustatic fluctuations were superimposed on tectonic subsidence and were largely re-  
 677 sponsible for changes on facies composition and distribution in the upper Frasnian and lower Fa-  
 678 mennian strata.

681 The correlations within the Canning Basin re-  
 682 fine the sequence stratigraphic framework. Our

transgressive interval across the Frasnian–Famennian boundary agrees with Canning Basin subsur-  
 683 face data (Kennard et al. (1992); Southgate et al., 1993) and some global sea level interpretations  
 684 (Hallam and Wignall, 1999). This transgression and corresponding positive  $\delta^{13}\text{C}$  excursion are  
 685 part of the ‘Frasnian–Famennian’ sequence of Kennard et al. (1992) (Fig. 9). The Frasnian low-  
 686 stand reef at the Oscar Range probably correlates with the lowstand reef tongue at the ‘classic face’  
 687 of Windjana Gorge (Whittam et al., 1994). The lower positive  $\delta^{13}\text{C}$  excursion and transgressive  
 688 interval correspond to Southgate et al.’s (1993) 691  
 692  
 693  
 694  
 695



1 Fig. 8. Late Devonian  $\delta^{13}\text{C}$  curves from Canning Basin compared to generalized carbon isotope curve from Europe (Joachimski  
 2 and Buggisch, 1993) and carbon isotope curve from Canada (Wang et al., 1996). The  $\delta^{13}\text{C}$  curve from Europe is plotted against  
 3 time.  $\delta^{13}\text{C}$  curves from Australia and Canada are plotted against thickness and adjusted so conodont dates correlate with the  
 4 European section. In conodont classification schemes, Frasnian biozone 13 is in upper *rhenana* to *linguiformis* biozones, and bio-  
 5 zone 12 is in lower to upper *rhenana* biozones (Klapper and Becker, 1998). Gap in Oscar Range curve is due to unconformity,  
 6 and placement of upper segment of this curve is uncertain. The generalized eustatic sea level curve is interpreted from Canning  
 7 Basin and European sections (Joachimski and Buggisch, 1993) and agrees with Hallam and Wignall’s (1999) interpretation. This  
 8 curve does not include possible short-term fluctuations in sea level, such as the one which may have occurred at the Frasnian–  
 9 Famennian boundary.



1 Fig. 9. Sequence stratigraphic interpretation based on Dingo Gap, Oscar Range, and Windjana Gorge stratigraphy and carbon  
 2 isotopic data. Section A is back-reef of Dingo Gap, section B is from Oscar Range, and section C is Windjana Gorge. Shaded  
 3 areas correspond to positive carbon isotope excursions. Sequence stratigraphic interpretation agrees with Kennard et al.'s (1992)  
 4 and Southgate et al.'s (1993) interpretations.

696 'Frasnian four' sequence (Fig. 9). Further correlations of these sequences within the Canning Basin and globally can be aided by additional use of  
 697 carbon isotope stratigraphy.  
 698  
 699

700 The Canning Basin shows some evidence for a drop in sea level at the Frasnian–Famennian boundary. At Windjana Gorge, a thin, 2-m, siltstone interval at the Frasnian–Famennian boundary may represent a drop in sea level. The siltstone and possible stromatolites at this interval may have been deposited as a function of sea-level-driven reciprocal sedimentation. This interval also may correspond to a stromatolite horizon at Dingo Gap, which George et al. (1997) interpret as a drop in sea level at the Frasnian–Famennian boundary. The negative  $\delta^{13}\text{C}$  excursion in the brachiopods just below the Frasnian–Famennian boundary in the 'classic face' of Windjana Gorge may be recording an isotopic shift associated with a short-term drop in sea level.

716 However, the drop in sea level at the Frasnian–Famennian boundary is interpreted as a short-term event superimposed on a broad transgression. Upper marginal slope facies at Windjana Gorge were not exposed at the Frasnian–Famennian boundary suggesting that the drop in sea

722 level was substantially less than the 150-m drop reported at the Frasnian–Famennian boundary in Canada (Mountjoy and Becker, 1996) and other locations around the world (Hallam and Wignall, 1999). At the Oscar Range, an erosional surface is present at the Frasnian–Famennian boundary (Playford et al., 1989). However, the upper positive  $\delta^{13}\text{C}$  excursion in the Oscar Range lies below the unconformity and is interpreted as entirely Frasnian based on the abundance of stromatopore fragments (Fig. 6). Since none of the positive  $\delta^{13}\text{C}$  excursion is Famennian, the lower Famennian, transgressive strata that contain the  $\delta^{13}\text{C}$  shift elsewhere in the basin must have been eroded away from the Oscar Range reef complex during a later drop in sea level during early Famennian time (Fig. 9). Thus, the sedimentological evidence in the Canning Basin suggests that the drop in sea level at the Frasnian–Famennian boundary was a short-term event superimposed on a third-order transgressive to highstand interval and was masked in shallow-water depositional environments by a greater drop in sea level which occurred during early Famennian time.

746 The correspondence of  $\delta^{13}\text{C}$  variations to inferred sea level changes suggests a dependence  
 747

of the Late Devonian carbon cycle on changes in ocean circulation and possibly climate. High  $\delta^{13}\text{C}$  values may reflect times of high organic carbon burial in continental and oceanic sediments (Joachimski and Buggisch, 1993; Wang et al., 1996; Joachimski et al., 2002). Density-stratified epeiric seas and other sedimentary basins produced black shales at several locations globally during Late Devonian time, especially during transgressions (Witzke and Heckel, 1988; Joachimski et al., 2001). By removing isotopically light organic carbon from the oceans, the dissolved inorganic carbon become isotopically heavier and become incorporated into calcite cements (Kump and Arthur, 1999; Joachimski et al., 2001). Alternatively by removing carbon dioxide from the atmosphere and oceans during burial of organic carbon, Late Devonian sea surface temperature probably decreased and pH of the oceans increased, possibly resulting in an increase in seawater  $\delta^{13}\text{C}$  values due to inorganic fractionation (Lynch-Stieglitz et al., 1995; Spero et al., 1997). During lowstands, destabilization or lowering of the pycnocline of these basins may have occurred due to changes in circulation or climate (Wignall, 1994; Joachimski et al., 2001). This may have resulted in the release and oxidation of isotopically light sedimentary organic carbon and methane clathrates, causing seawater  $\delta^{13}\text{C}$  values to return to baseline levels (Buggisch, 1991; Haq, 1998).

## 6. Conclusion

In conjunction with biostratigraphy and sequence stratigraphy, carbon isotope stratigraphy provides a powerful tool for correlating upper Frasnian and lower Famennian strata and is especially useful in shallow-water reef environments, where biostratigraphic data are typically lacking. Fluctuations in global carbon isotopic values are a function of a sea-level-driven carbon cycle, and positive  $\delta^{13}\text{C}$  excursions correspond to eustatic highs. At Windjana Gorge, reciprocal carbonate–siliciclastic sedimentation was driven by eustatic sea level changes, and based on positive  $\delta^{13}\text{C}$  excursions, carbonate-rich intervals at

Windjana Gorge correlate to other transgressive interval in the Canning Basin and Europe. Carbon isotope stratigraphy also reveals the correlation between lowstand reefs in the Oscar Range with siliciclastic deposition at Windjana Gorge. A minor drop in sea level probably occurred at the Frasnian–Famennian boundary, which was eroded from shallow-water reef environments by a greater drop in sea level during early Famennian time. Based on biostratigraphy, sequence stratigraphy, and carbon isotope stratigraphy, correlations in the Canning Basin help develop a sequence stratigraphic model, from which other upper Frasnian–lower Famennian sections can be compared.

## 7. Uncited references

Racki, 1999; Spero, 1992

## Acknowledgements

We thank Phil Playford for his invaluable assistance in the field. Sarah Tourre, Nancy Slatter, and Marie Reil were very capable field assistants. Isotopic analyses were performed in the laboratory of Dr. Howard Spero at the University of California at Davis. We thank the Western Australian Bureau of Conservation and Land Management (CALM) for permission to collect samples from state lands and the Kimberley Diamond Company for use of roads leading to the Oscar Range. Dave Osleger, Jay Kaufman, Lee Kump, Annette George, Isabel Montanez, Howard Spero, and Michael Joachimski provided useful comments on an earlier version of the manuscript. Acknowledgment is made to the donors of The Petroleum Research Fund, administered by the ACS, for partial support of this research. Funding for this project was also provided by the UC-Davis Durrell Memorial Fund, the SEPM Weimar Student Grant, the University Research Expedition Program (UREP), and the AAPG Grants-in-Aid Fund. We thank UREP participants: James Bishop, Sabina Pan, Nate Patterson, RoseMary Natelson, Doris Beaman,



- 16 *N.P. Stephens, D.Y. Sumner / Palaeogeography, Palaeoclimatology, Palaeoecology 3024 (2002) 1–17*
- 835 Liza Coe, Tania Bricker-Shanahan, and Shane  
836 McQuade.
- 837 **References**
- 838 Becker, R.T., House, M.R., 1997. Sea-level changes in the  
839 Upper Devonian of the Canning Basin, Western Australia.  
840 *Cour. Forsch.-Inst. Senckenberg* 199, 129–146.
- 841 Becker, R.T., House, M.R., Kirchgasser, W.T., 1993. Devoni-  
842 an goniatite biostratigraphy and timing of facies movements  
843 in the Frasnian of the Canning Basin, Western Australia.  
844 In: Hailwood, E.A., Kidd, R.B. (Eds.), *High Resolution*  
845 *Sequence Stratigraphy*. *Geol. Soc. Spec. Publ.* 70, 293–321.
- 846 Becker, R.T., House, M.R., Kirchgasser, W.T., Playford, P.P.,  
847 1991. Sedimentary and faunal changes across the Frasnian/  
848 Famennian boundary in the Canning Basin of Western Aus-  
849 tralia. *Hist. Biol.* 5, 183–196.
- 850 Brown, S.A., Boserio, I.M., Jackson, K.S., Spence, K.W.,  
851 1984. The geological evolution of the Canning Basin – Im-  
852 plications for petroleum exploration. In: Purcell, P.G. (Ed.),  
853 *The Canning Basin*, W.A. Geological Society of Australia,  
854 pp. 85–96.
- 855 Buggisch, W., 1991. The global Frasnian–Famennian ‘Kell-  
856 wasser Event’. *Geol. Rundsch.* 80, 49–72.
- 857 Carpenter, S.J. et al., 1991.  $\delta^{18}\text{O}$  values,  $^{87}\text{Sr}/^{86}\text{Sr}$  and  $\text{Sr}/\text{Mg}$   
858 ratios of Late Devonian abiotic marine calcite: Implications  
859 for the composition of ancient seawater. *Geochim. Cosmo-*  
860 *chim. Acta* 55, 1991–2010.
- 861 Copper, P., 1986. Frasnian/Famennian mass extinction and  
862 cold-water oceans. *Geology* 14, 835–839.
- 863 Ferreri, V., 1997. Carbon isotope stratigraphy: a tool for basin  
864 to carbonate platform correlation. *Terra Nova* 9, 57–61.
- 865 Geldsetzer, H.H.J., Goodfellow, W.D., McLaren, D.J., 1993.  
866 The Frasnian–Famennian extinction event in a stable cratonic  
867 shelf setting: Trout River, Northern Territories, Can-  
868 ada. *Palaeogeogr. Palaeoclimatol. Palaeoecol.* 104, 81–95.
- 869 George, A.D., 1999. Deep-water stromatolites, Canning Basin,  
870 Northwestern Australia. *Palaios* 14, 493–505.
- 871 George, A.D., Chow, N., 2002. The depositional record of the  
872 Frasnian/Famennian boundary interval in a fore-reef succes-  
873 sion, Canning Basin, Western Australia. *Palaeogeogr. Palae-*  
874 *oclimatol. Palaeoecol.* 181, 347–374.
- 875 George, A.D., Playford, P.E., Powell, C.M., Tornatora, P.M.,  
876 1997. Lithofacies and sequence development on an Upper  
877 Devonian mixed carbonate-siliciclastic fore-reef slope, Can-  
878 ning Basin, Western Australia. *Sedimentology* 44, 843–867.
- 879 Grotsch, J., Billing, I., Vahrenkamp, V., 1998. Carbon-isotope  
880 stratigraphy in shallow-water carbonates: implications for  
881 Cretaceous black-shale deposition. *Sedimentology* 45, 623–  
882 634.
- 883 Guppy, D.J., Lindner, A.W., Rattigan, J.H., Casey, J.N.,  
884 1958. The geology of the Fitzroy Basin, Western Australia.  
885 *Bur. Min. Resources Geol. Geophys. Western Australia*  
886 *Bull.* 36, 1–73.
- 887 Hall, W.D.M., 1984. The stratigraphy and structural develop-  
ment of the Givetian-Frasnian Reef Complex, Limestone  
Billy Hills, Western Pillara Range, W.A. In: Purcell, P.G.  
(Ed.), *The Canning Basin*, W.A. *Proceeding of Geol. Soc.*  
890 *Aust./Pet. Explor. Soc. Aust. Symposium*, Perth, pp. 215–  
891 222.
- 892 Hallam, A., Wignall, P.B., 1999. Mass extinctions and sea-level  
893 changes. *Earth-Sci. Rev.* 48, 217–250.
- 894 Handford, C.R., Loucks, R.G., 1993. Carbonate deposition  
895 sequences and systems tracts – Responses of carbonate plat-  
896 forms to relative sea-level changes. In: Loucks, R.G., Sarg,  
897 J.F. (Eds.), *Carbonate Sequence Stratigraphy*. *AAPG Mem.*  
898 57, 3–41.
- 899 Haq, B.U., 1998. Natural gas hydrates: searching for the long-  
900 term climatic and slope-stability records. In: Henriot, J.P.,  
901 Mienert, J. (Eds.), *Gas Hydrates: Relevance to World Mar-*  
902 *gin Stability and Climate Change*. *Geol. Soc. London Spec.*  
903 *Publ.* 137, 303–318.
- 904 Hoffman, P.F., Kaufman, A.J., Halverson, G.P., Schrag, D.P.,  
905 1998. A Neoproterozoic snowball earth. *Science* 281, 1342–  
906 1346.
- 907 Holmes, A.E., Christie-Blick, N., 1993. Origin of sedimentary  
908 cycles in mixed carbonate-siliciclastic systems: An example  
909 from the Canning Basin, Western Australia. In: Loucks,  
910 R.G., Sarg, J.F. (Eds.), *Carbonate Sequence Stratigraphy*.  
911 *AAPG Mem.* 57, 181–212.
- 912 Hurley, N.F., 1986. Geology of the Oscar Range Devonian  
913 Reef Complex, Canning Basin, Western Australia. Ph.D  
914 Thesis, University of Michigan, Ann Arbor, MI.
- 915 Hurley, N.F., Lohmann, K.C., 1989. Diagenesis of Devonian  
916 reefal carbonates in the Oscar Range, Canning Basin, West-  
917 ern Australia. *J. Sediment. Petrol.* 59, 127–146.
- 918 Joachimski, M.M., Buggisch, W., 1993. Anoxic events in the  
919 late Frasnian – Causes of the Frasnian–Famennian faunal  
920 crisis? *Geology* 21, 675–678.
- 921 Joachimski, M.M., Ostertag-Henning, C., Pancost, R.D.,  
922 Strauss, H., Freeman, K.H., Littke, R., Sinninghe Damste,  
923 J.S., Racki, G., 2001. Water column anoxia, enhanced pro-  
924 ductivity and concomitant changes in  $\delta^{13}\text{C}$  and  $\delta^{34}\text{S}$  across  
925 the Frasnian–Famennian boundary, Kowala–Holy Cross  
926 Mountains, Poland. *Chem. Geol.* 175, 109–131.
- 927 Joachimski, M.M., Pancost, R.D., Freeman, K.H., Ostertag-  
928 Henning, C., Buggisch, W., 2002. Carbon isotope geochem-  
929 istry of the Frasnian–Famennian transition. *Palaeogeogr.*  
930 *Palaeoclimatol. Palaeoecol.* 181, 91–109.
- 931 Kaufman, A.J., Knoll, A.H., 1995. Neoproterozoic variations  
932 in the C-isotopic composition of seawater: stratigraphic and  
933 biogeochemical implications. *Precambrian Res.* 73, 27–49.
- 934 Kennard, J.M., Southgate, P.N., Jackson, M.J., O’Brien, P.E.,  
935 Christie-Blick, N., Holmes, A.E., Sarg, J.F., 1992. New se-  
936 quence perspective on the Devonian reef complex and the  
937 Frasnian–Famennian boundary, Canning Basin, Australia.  
938 *Geology* 20, 1135–1138.
- 939 Kenter, J.A.M., Ginsburg, R.N., Troelstra, S.R., 2001. Sea-  
940 level-driven sedimentation patterns on the slope and margin.  
941 In: Ginsburg, R.N. (Ed.), *Subsurface Geology of a Prograd-*  
942 *ing Carbonate Platform Margin, Great Bahama Bank: Re-*  
943

- 944 sults of the Bahamas Drilling Program. *SEPM Spec. Publi.*  
945 30, 61–100.
- 946 Kerans, C., Hurley, N.F., Playford, P.E., 1986. Marine dia-  
947 genesis in Devonian reef complexes of the Canning Basin,  
948 Western Australia. In: Schroeder, J.H., Purser, B.H. (Eds.),  
949 Reef Diagenesis. Springer-Verlag, Heidelberg, pp. 357–380.
- 950 Klapper, G., Becker, R.T., 1998. Comparison of Frasnian  
951 (Upper Devonian) conodont zonations. In: Bagnoli, G.  
952 (Ed.), Seventh International Conodont Symposium Held in  
953 Europe (ECOS VII), abstracts, pp. 53–54.
- 954 Kump, L.R., 1991. Interpreting carbon-isotope excursions:  
955 Strangelove oceans. *Geology* 19, 299–302.
- 956 Kump, L.R., Arthur, M.A., 1999. Interpreting carbon-isotope  
957 excursions: carbonates and organic matter. *Chem. Geol.*  
958 161, 181–198.
- 959 Lynch-Stieglitz, J., Stocker, T.F., Broecker, W.S., Fairbanks,  
960 R.G., 1995. The influence of air-sea exchange on the isotopic  
961 composition of oceanic carbon: Observations and modeling.  
962 *Global Biogeochem. Cycles* 9, 653–665.
- 963 Mountjoy, E.W., Becker, S., 1996. A major sea-level fall at end  
964 of Frasnian (Upper Devonian) and rapid filling of the Jasper  
965 Basin, Sassenach Formation, Alberta Rocky Mountains.  
966 Abstracts, AAPG and SEPM Annual Meeting 5, 102.
- 967 Nicoll, R.S., 1984. Conodont distribution in the marginal-  
968 slope facies of the Upper Devonian reef complex, Canning  
969 Basin, Western Australia. *Geol. Soc. Am. Spec. Pap.* 196,  
970 127–141.
- 971 Playford, P.E., 1980. Devonian ‘Great Barrier Reef’ of Canning  
972 Basin, Western Australia. *AAPG Bull.* 62, 814–841.
- 973 Playford, P.E., Hocking, R.M., 1999. Devonian reef complexes  
974 of the Canning Basin: Geological Survey of Western Aus-  
975 tralia: geologic maps of the Lennard Shelf (Plates 1–7) to  
976 accompany bulletin 145 (in preparation).
- 977 Playford, P.E., Lowry, D.C., 1966. Devonian reef complexes  
978 of the Canning Basin, Western Australia. *Western Australia*  
979 *Geol. Surv. Bull.* 118, 1–150.
- 980 Playford, P.E., McLaren, D.J., Orth, C.J., Gilmore, J.S.,  
981 Goodfellow, W.D., 1984. Iridium anomaly in the Upper De-  
982 vonian of the Canning Basin, Western Australia. *Science*  
983 226, 437–439.
- 984 Playford, P.E., Hurley, N.F., Middleton, M.F., 1989. Reefal  
985 platform development, Devonian of the Canning Basin,  
986 Western Australia. Controls on carbonate platform and ba-  
987 sin development. *SEPM Spec. Publ.* 44, 187–202.
- 988 Read, J.F., 1973. Carbonate cycles, Pillara Formation (Devo-  
989 nian), Canning Basin, Western Australia. *Bull. Can. Pet.*  
990 *Geol.* 21, 38–51.
- 991 Racki, G., 1999. The Frasnian–Famennian biotic crisis: How  
992 many (if any) bolide impacts? *Geol. Rundsch.* 87, 617–632.
- Sepkoski, J.J., 1996. Patterns of Phanerozoic extinction: a  
perspective from global data bases. In: Walliser, O.H.  
(Ed.), *Global Events and Event Stratigraphy in the Phaner-*  
*ozoic.* Springer, Berlin, pp. 35–51.
- Southgate, P.N., Kennard, J.M., Jackson, M.J., O’Brien, P.E.,  
Sexton, M.J., 1993. Reciprocal lowstand clastic and high-  
stand carbonate sedimentation, subsurface, Devonian Reef  
Complex, Canning Basin, Western Australia. In: Loucks,  
R.G., Sarg, J.F. (Eds.), *Carbonate Sequence Stratigraphy.*  
*AAPG Mem.* 57, 157–179.
- Spero, H.J., 1992. Do planktic foraminifera accurately record  
shifts in the carbon isotopic composition of seawater  $\epsilon\text{CO}_2$ ?  
*Mar. Micropaleontol.* 19, 275–285.
- Spero, H.J., Lea, D.W., 2002. The cause of carbon isotope  
minimum events on glacial terminations. *Science* 296, 522–  
525.
- Thompson, J.B., Newton, C.R., 1988. Late Devonian mass  
extinction: Episodic climatic cooling or warming. In: Mc-  
Millan, N.J. (Ed.), *Devonian of the World, Volume III.*  
*Can. Soc. Pet. Geol. Mem.* 14, 29–34.
- Wang, K., Geldsetzer, H.H.J., Goodfellow, W.D., Krouse,  
H.R., 1996. Carbon and sulfur isotope anomalies across  
the Frasnian–Famennian extinction boundary, Alberta,  
Canada. *Geology* 24, 187–191.
- Ward, W.B., 1999. Tectonic control on backstepping sequen-  
ces revealed by mapping of Frasnian backstepped platforms,  
Devonian Reef Complexes, Napier Range, Canning Basin,  
Western Australia. In: Harris, P.M., Saller, A.H., Simo,  
J.A. (Eds.), *Advances in Carbonate Sequence Stratigraphy:*  
*Applications to Reservoirs, Outcrops, and Models.* *SEPM*  
*spec. Publ.* 63, 47–74.
- Whittam, D.B., Kennard, J.M., Kirk, R.B., Sarg, J.F., South-  
gate, P.N., 1994. A proposed third-order sequence frame-  
work for the Upper Devonian outcrops of the Northern  
Canning Basin. In: Purcell, P.G., Purcell, R.R. (Eds.), *Pro-*  
*ceedings of the West Australian Basins Symposium.* *Petro-*  
*leum Exploration Society of Australia, Perth, WA,* pp. 697–  
702.
- Wignall, P.B., 1994. *Black Shales.* Clarendon Press, Oxford, 127  
pp.
- Witzke, B.J., Heckel, P.H., 1988. Paleoclimatic indicators and  
inferred Devonian paleolatitudes of Euramerica. In: McMil-  
lan, N.J. (Ed.), *Devonian of the World, vol. 1.* *Can. Soc.*  
*Pet. Geol.* 49–63.
- Wood, R., 2000. Palaeoecology of a Late Devonian back reef,  
Canning Basin, Western Australia. *Palaeontology* 43, 671–  
703.